# The scalar, vector and tensor contributions of a stochastic background of magnetic fields to CMB anisotropies

D. Paoletti $^{\star 1,2}$, F. Finelli $^{\dagger 2,3,4}$ and F. Paci $^{\ddagger 5,2,4}$

$^1$ *Dip. di Fisica, Università degli studi di Ferrara and INFN,*
*via Saragat 1, I-44100 Ferrara - Italy*
$^2$ *INAF-IASF Bologna, Istituto di Astrofisica Spaziale e Fisica Cosmica di Bologna*
*Istituto Nazionale di Astrofisica, via Gobetti 101, I-40129 Bologna - Italy*
$^3$ *INAF-OAB, Osservatorio Astronomico di Bologna*
*Istituto Nazionale di Astrofisica, via Ranzani 1, I-40127 Bologna - Italy*
$^4$ *INFN, Sezione di Bologna, Via Irnerio 46, I-40126 Bologna, Italy*
$^5$ *Dipartimento di Astronomia, Università degli Studi di Bologna,*
*via Ranzani, 1 – I-40127 Bologna – Italy*

22 May 2009

**ABSTRACT**

We study the contribution of a stochastic background (SB) of primordial magnetic fields (PMF) on the anisotropies in temperature and polarization of the cosmic microwave background radiation (CMB). A SB of PMF modelled as a fully inhomogeneous component induces non-gaussian scalar, vector and tensor metric linear perturbations. We give the exact expressions for the Fourier spectra of the relevant energy-momentum components of such SB, given a power-law dependence parametrized by a spectral index $n_B$ for the magnetic field power spectrum cut at a damping scale $k_D$. For all the values of $n_B$ considered here, the contribution to the CMB temperature pattern by such a SB is dominated by the scalar contribution and then by the vector one at higher multipoles. We also give an analytic estimate of the scalar contribution to the CMB temperature pattern.

**Key words:** Cosmology: cosmic microwave background – Physical data and processes: magnetic fields.

## 1 INTRODUCTION

The origin of the large scale magnetic fields observed is an issue of great importance in astrophysics (see Subramanian (2006) for a review). Primordial magnetic fields (PMF) generated in the early Universe are a possible explanation of large scale magnetic fields in clusters of galaxies and galaxies and might have left an imprint in the anisotropy pattern of the cosmic microwave background (CMB) (see Durrer (2007) for a review).

$^\star$ paoletti@iasfbo.inaf.it
$^\dagger$ finelli@iasfbo.inaf.it
$^\ddagger$ paci@iasfbo.inaf.it

A stochastic background (SB) is the simplest way to model these random PMFs in an isotropic and homogeneous background. A SB of PMF is modelled as a fully inhomogeneous component and its energy momentum tensor (EMT) - quadratic in the magnetic fields - is considered at the same footing as linear inhomogeneities in the other components and linear metric fluctuations. A SB of PMF generates independent modes for all kinds of linear perturbations: there has been several studies for scalar (Koh and Lee (2000); Kahniashvili and Ratra (2006); Giovannini and Kunze (2008) and references therein; Finelli, Paci & Paoletti 2008 - henceforth FPP -), vector (Subramanian and Barrow

1998;       Seshadri and Subramanian       2001;
Mack, Kahniashvili and Kosowsky       2002;       Lewis
2004) and tensor (Durrer, Ferreira and Kahniashvili
2000;       Mack, Kahniashvili and Kosowsky       2002;
Caprini, Durrer and Kahniashvili 2004) perturbations
in presence of a SB of PMF. Limits on the amplitude
and spectral index of the PMF were also obtained by an
exploration of a flat ΛCDM model in presence of such
SB (Yamazaki, Ichiki, Kajino and Mathews 2006).

We study the problem by a numerical Eistein-Boltzmann code extending the results obtained in our
previous work (FPP). The study of the impact of a
SB of PMF on CMB anisotropies requires a detailed
study of the initial conditions for fluctuations and of
the power spectra of the EMT of the SB of PMF.
Our paper improves previous results in these two as-
pects. In this paper we obtain the Fourier spectra
of the relevant vector and tensor energy-momentum
components of the SB of PMF along the procedure
used in FPP for the scalar components. As shown in
FPP, by solving exactly the convolution integrals for
a sequence of values for the spectral slope $n_B$ which
parametrizes the PMF power spectrum, previous results
of Mack, Kahniashvili and Kosowsky (2002) may be sig-
nificantly improved.

With these improved correlators we then investi-
gate the impact of a stochastic background of primordial
magnetic fields on scalar, vector and tensor cosmolog-
ical perturbations and in particular on CMB temper-
ature and polarization anisotropies. Our results show
that it is very important to study also vector perturba-
tions since these dominate at high $\ell$ over the scalar ones
for any slope of the spectrum of PMF.

Our paper is organized as follows. In Section 2 we
introduce our conventions for a non-helical SB and the
scalar, vector and tensor decomposition of its EMT:
we give our exact results for the relevant objects for
a set of $n_B$ leaving the details in Appendices A, B,
and we show how our exact results improve on pre-
vious results. The set of $n_B$ now includes also values
$n_B < -3/2$ which were not studied in FPP. Section
3 presents the decomposition of metric perturbations
and sections 4,5,6 present the study of scalar, vector
and tensor cosmological perturbations in presence of a
SB of PMF, respectively. In Section 7 we present the
results obtained by our modified version of the CAMB
code (Lewis,Challinor and Lasenbly 2000). We conclude
in Section 8.

## 2   STOCHASTIC BACKGROUND OF PRIMORDIAL MAGNETIC FIELDS

Since the EMT of PMF at homogeneous level is zero, at
linear order PMFs evolve like a stiff source and there-
fore it is possible to discard the back-reaction of gravity
onto the SB of PMF. Before the decoupling epoch the
electric conductivity of the primordial plasma is very
large, therefore it is possible at lowest order to con-
sider the infinite conductivity limit, in which the in-
duced electric field is zero. Within the infinite conduc-
tivity limit the magnetic field amplitude scales simply
as $\mathbf{B}(\mathbf{x}, \tau) = \mathbf{B}(\mathbf{x})/a(\tau)^2$ and [1] the EMT of a SB of
PMF is:

$$\tau_0^0 \;=\; -\rho_B = -\frac{B^2(\mathbf{x})}{8\pi a^4(\tau)} \tag{2.1}$$

$$\tau_i^0 \;=\; 0 \tag{2.2}$$

$$\tau_j^i \;=\; \frac{1}{4\pi a^4(\tau)}\Big(\frac{B^2(\mathbf{x})}{2}\delta_j^i - B_j(\mathbf{x})B^i(\mathbf{x})\Big) \tag{2.3}$$

The two point correlation function in the Fourier space
[2] for fully inhomogeneous fields is:

$$\langle B_i(\mathbf{k})B_j^*(\mathbf{k}')\rangle = (2\pi)^3\delta(\mathbf{k} - \mathbf{k}')(\delta_{ij} - \hat{k}_i\hat{k}_j)\frac{P_B(k)}{2} \tag{2.4}$$

Where $P_B(k)$ is the spectrum of PMF parametrized as:

$$P_B(k) = A\Big(\frac{k}{k_*}\Big)^{n_B}, \tag{2.5}$$

and $k_*$ is a reference scale. PMF are damped on small
scales by radiation viscosity. We model this damping
introducing a sharp cut-off in the PMF power spectrum
at a damping scale called $k_D$. The relation between the
amplitude of PMF power spectrum and the amplitude
of the field itself is:

$$\langle B^2\rangle \;=\; \langle B_i^*(\mathbf{x}')B_i(\mathbf{x})\rangle|_{\mathbf{x}'=\mathbf{x}}$$
$$=\; \frac{1}{2\pi^2}\int_0^{k_D} dk\, k^2 P_B(k) \tag{2.6}$$

Solving the integral above we obtain:

$$\langle B^2\rangle = \frac{A}{2\pi^2(n_B + 3)}\frac{k_D^{n_B+3}}{k_*^{n_B}}, \tag{2.7}$$

where for the convergence of the integral above is re-
quested $n_B > -3$. We shall use to denote the magnetic
field amplitude this quantity instead of smearing the
field at an additional scale $\lambda$, as in FPP:

$$\langle B^2\rangle_\lambda = \frac{1}{2\pi}\int dk k^2 P_B(k) e^{-\lambda^2 k^2} \tag{2.8}$$

---

[1] We choose the standard convention in which at present
time $t_0$, $a(t_0) = 1$.
[2] As Fourier transform and its inverse, we use:

$$Y(\mathbf{k}, \tau) \;=\; \int d\mathbf{x} e^{i\mathbf{k}\cdot\mathbf{x}} Y(\mathbf{x}, \tau)$$

$$Y(\mathbf{x}, \tau) \;=\; \int \frac{d\mathbf{k}}{(2\pi)^3} e^{-i\mathbf{k}\cdot\mathbf{x}} Y(\mathbf{k}, \tau)\,.$$

where $Y$ is a generic function. Note that we have changed
our Fourier conventions with respect to FPP.

The two definitions can however related simply by:

$$\langle B^2 \rangle = \langle B^2 \rangle_\lambda \frac{k_D^{n_B+3}\lambda^{n_B+3}}{(n_B+3)\Gamma\left(\frac{n_B+3}{2}\right)} \qquad (2.9)$$

The EMT of PMF is quadratic in the magnetic field and therefore its Fourier transfom is a convolution. The two point correlation function of the spatial part of EMT is[3]:

$$\langle \tau_{ab}^*(\mathbf{k})\tau_{cd}(\mathbf{k}')\rangle = \int \frac{d\mathbf{q}d\mathbf{p}}{64\pi^5}\delta_{ab}\delta_{cd}\langle B_l(\mathbf{q})B_l(\mathbf{k}-\mathbf{q})B_m(\mathbf{p})B_m(\mathbf{k}'-\mathbf{p})\rangle/2$$
$$- \int \frac{d\mathbf{q}d\mathbf{p}}{32\pi^5}\langle B_a(\mathbf{q})B_b(\mathbf{k}-\mathbf{q})B_c(\mathbf{p})B_d(\mathbf{k}'-\mathbf{p})\rangle/2$$

We can then obtain scalar, vector and tensor correlation functions:

$$\langle \Pi^{*(S)}(\mathbf{k})\Pi^{(S)}(\mathbf{k}')\rangle = \delta_{ab}\delta_{cd}\langle\tau_{ab}^*(\mathbf{k})\tau_{cd}(\mathbf{k}')\rangle$$
$$\langle \Pi_i^{*(V)}(\mathbf{k})\Pi_j^{(V)}(\mathbf{k}')\rangle = k_a P_{ib}(\mathbf{k})k_c' P_{jd}(\mathbf{k}')\langle\tau_{ab}^*(\mathbf{k})\tau_{cd}(\mathbf{k}')\rangle$$
$$\langle \Pi_{ij}^{*(T)}(\mathbf{k})\Pi_{tl}^{(T)}(\mathbf{k}')\rangle = (P_{ia}(\mathbf{k})P_{jb}(\mathbf{k}) - \frac{1}{2}P_{ij}(\mathbf{k})P_{ab}(\mathbf{k})) \times$$
$$(P_{tc}(\mathbf{k}')P_{ld}(\mathbf{k}') - \frac{1}{2}P_{tl}(\mathbf{k}')P_{cd}(\mathbf{k}'))\langle\tau_{ab}^*(\mathbf{k})\tau_{cd}(\mathbf{k}')\rangle , \quad (2.10)$$

where $P_{ij} = \delta_{ij} - \hat{k}_i\hat{k}_j$. Such convolutions can be written in terms of spectra as follows:

$$\langle \Pi^{*(S)}(\mathbf{k})\Pi^{(S)}(\mathbf{k}')\rangle = |\Pi^{(S)}(k)|^2\delta(\mathbf{k}-\mathbf{k}')$$
$$\langle \Pi_i^{*(V)}(\mathbf{k})\Pi_j^{(V)}(\mathbf{k}')\rangle = \frac{1}{2}|\Pi^{(V)}(k)|^2 P_{ij}(\mathbf{k})\delta(\mathbf{k}-\mathbf{k}')$$
$$\langle \Pi_{ij}^{*(T)}(\mathbf{k})\Pi_{tl}^{(T)}(\mathbf{k}')\rangle = \frac{1}{4}|\Pi^{(T)}(k)|^2\mathcal{M}_{ijtl}(\mathbf{k})\delta(\mathbf{k}-\mathbf{k}')$$

where $\mathcal{M}_{ijtl} = P_{it}P_{jl} + P_{il}P_{jt} - P_{ij}P_{tl}$. With this choice the spectra take the form:

$$|\rho_B(k)|^2 = \frac{1}{1024\pi^5}\int d\mathbf{p}P_B(p)\,P_B(|\mathbf{k}-\mathbf{p}|)(1+\mu^2) \quad (2.11)$$

$$|\Pi^{(V)}(k)|^2 = \frac{1}{512\pi^5}\int d\mathbf{p}P_B(p)\,P_B(|\mathbf{k}-\mathbf{p}|) \times$$
$$[(1+\beta^2)(1-\gamma^2) + \gamma\beta(\mu-\gamma\beta)] \quad (2.12)$$

$$|\Pi^{(T)}(k)|^2 = \frac{1}{512\pi^5}\int d\mathbf{p}P_B(p)\,P_B(|\mathbf{k}-\mathbf{p}|) \times$$
$$(1 + 2\gamma^2 + \gamma^2\beta^2) , \quad (2.13)$$

where $\mu = \hat{\mathbf{p}}\cdot(\mathbf{k}-\mathbf{p})/|\mathbf{k}-\mathbf{p}|$, $\gamma = \hat{\mathbf{k}}\cdot\hat{\mathbf{p}}$, $\beta = \hat{\mathbf{k}}\cdot(\mathbf{k}-\mathbf{p})/|\mathbf{k}-\mathbf{p}|$. These equations agree, within our Fourier convention, with previous results by Mack, Kahniashvili and Kosowsky (2002), Durrer, Ferreira and Kahniashvili (2000). One of the main results of our work is the calculation of the correct, i.e. without any approximation, expressions for these convolutions, given a power spectrum as in Eq.(2.5) with a sharp cut-off at $k_D$.

---

[3] We use the convention that latin indexes run from 1 to 3 while greek indexes run from 0 to 3

In the appendices we explain the integration technique and show the results for various spectral indexes $n_B = 3, 2, 1, 0, -1, -3/2, -5/2$: in this paper we add $n_B = -5/2$ to the previously studied $n_B \geq -3/2$ values for scalar quantities studied in FPP. As for the scalar energy density and Lorentz force discussed in FPP, also the vector and tensor anisotropic stresses have support for Fourier modes with modulus smaller than $2k_D$. We show in Figure 1 the behaviour of scalar, vector and tensor quantities for $n_B = 2, -5/2$, respectively. For $n_B = -5/2$ the spectra for $k \ll k_D$ is:

$$|\rho(k)|^2_{n_B=-5/2} \simeq \frac{17A^2 k_*^5}{800\pi^4 k^2} \qquad (2.14)$$

whose slope, but not the amplitude, agrees with Kahniashvili and Ratra (2006). For $n_B = -5/2$, $|L(k)|^2 \simeq (55/51)|\rho(k)|^2$ for $k \ll k_D$ (for $n_B \geq -3/2$ we obtained $|L(k)|^2 \simeq (11/15)|\rho(k)|^2$ for $k \ll k_D$ FPP). Note also how the tensor contribution dominates over other ones in amplitude of the Fourier spectra, in agreement with previous numerical findings (Brown and Crittenden 2005).

The vector and tensor anisotropic stresses are shown with varying $n_B$ in Figure 2. The vector and tensor contributions have a $k$-dependence very similar to the energy-density: for $k \ll k_D$ and $n_B > -3/2$ ($n_B = -3/2$) $|\Pi^{(V)}(k)|^2, |\Pi^{(T)}(k)|^2$ have a white noise (logarithmic divergent) spectrum with $|\Pi^{(T)}(k)|^2 \simeq 2|\Pi^{(V)}(k)|^2$, whereas for $n_B = -5/2$ both become infrared dominated as $|\Pi^{(T)}(k)|^2 \simeq (94/25)|\Pi^{(V)}(k)|^2$ holds. The generic behaviour of $|\Pi^{(V)}(k)|^2$ for $k \ll k_D$ and $n_B > -3/2$ is:

$$|\Pi^{(V)}(k)|^2 \simeq \frac{A^2 k_D^{2n+3}}{256\pi^4 k_*^{2n}(3+2n_B)}\frac{28}{15} . \qquad (2.15)$$

The pole for $n_B = -3/2$ in Eq. (2.15) is replaced by a logarithmic diveregence in $k$ in the exact result reported in the Appendix A; the result reported by Mack, Kahniashvili and Kosowsky (2002) has a factor 4 instead of the factor 56/15 reported in Eq. (2.15). Note also that the relation between the tensor and vector anisotropic stresses is different from the one reported in Mack, Kahniashvili and Kosowsky (2002), who predict (in our conventions): $|\Pi^{(T)}(k)|^2 = |\Pi^{(V)}(k)|^2$, this relation is obtained neglecting the angular part in Eqs.(2.12,2.13) and is incorrect.

# 3 PERTUBATIONS EVOLUTION WITH PMF

The presence of PMF influences the cosmological perturbations evolution mainly in three ways. PMFs carry energy and momentum at the perturbation level and therefore gravitate, influencing the metric perturbations. As a second point, they carry anisotropic stress, which adds to the ones already present in the plasma
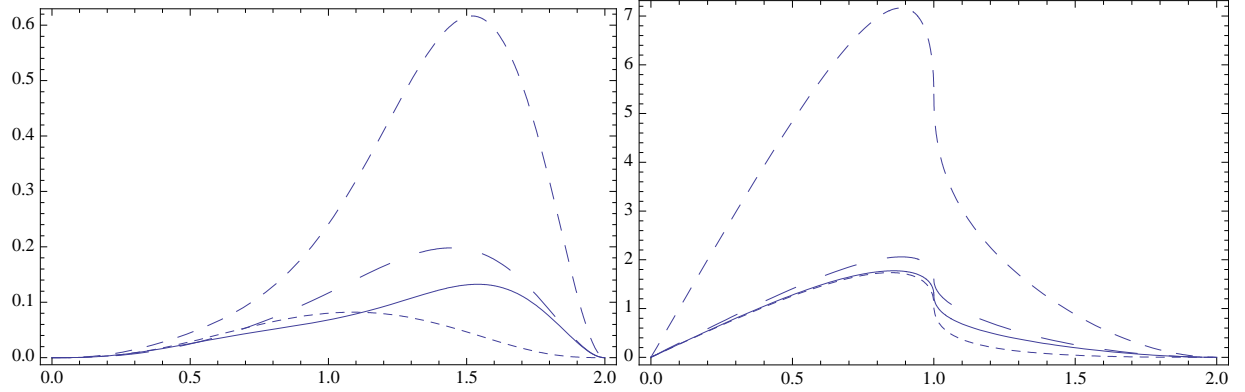
**Figure 1.** Comparison of $k^3|\rho_B(k)|^2$ (solid line), $k^3|L(k)|^2$ (large dashed line) $k^3|\Pi_i^{(V)}(k)|^2$ (small dashed line), $k^3|\Pi_{ij}^{(T)}(k)|^2$ (medium dashed line) in units of $\langle B^2\rangle^2/(1024\pi^3)$ versus $k/k_D$. The left and right panel are for $n_B = 2$ and $n_B = -5/2$, respectively.
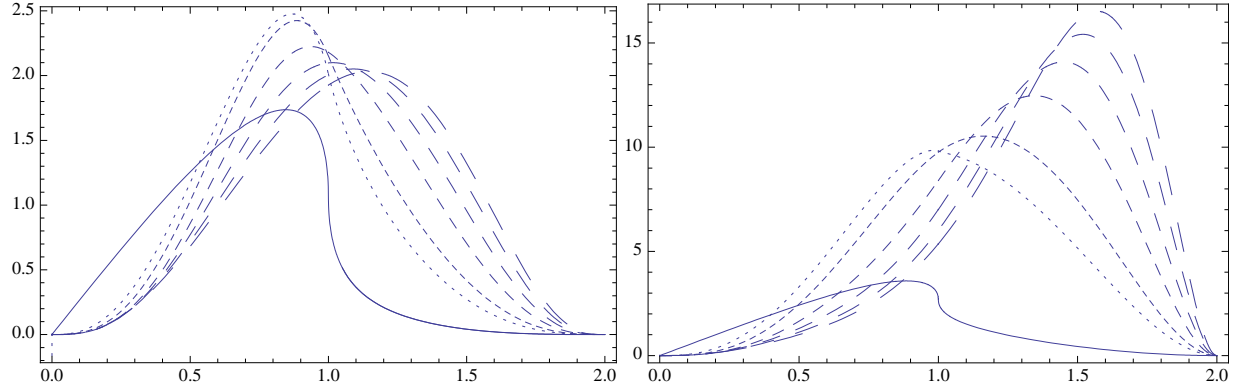


**Figure 2.** Plot of $k^3|\Pi^{(V)}(k)|^2$ (left panel) and $k^3|\Pi^{(T)}(k)|^2$ (right panel) in units of $\langle B^2\rangle^2/(1024\pi^3)$ versus $k/k_D$ for different $n_B$ for fixed $\langle B^2\rangle$. The different lines are for $n_B = -5/2, -3/2, -1, 0, 1, 2, 3$ ranging from the solid to the longest dashed.

given by neutrinos and photons, with the caveat that the photon anisotropic stress is negligible before decoupling epoch. Third, the presence of PMF induces a Lorentz force on baryons, which modifies their velocity. Due to the tight coupling between photons and baryons prior to the decoupling epoch the Lorentz force has an indirect effect also on photons during this regime.

The evolution of metric perturbations is described by the Einstein equations. These are modified by the presence of PMFs that represent a source term as follows:

$$G_{\mu\nu} = 8\pi(T_{\mu\nu} + \tau_{\mu\nu}),\qquad(3.16)$$

where as usual $\tau_{\mu\nu}$ represents the PMF EMT. The metric chosen in this work is:

$$ds^2 = a^2(\tau)\left[-d\tau^2 + (\delta_{ij} + h_{ij})\,dx^i dx^j\right]\qquad(3.17)$$

where $h_{ij}$ can be decomposed into a trace part $h$ and a traceless part consisting of its scalar, vector and tensor

part (Ma and Bertschinger 1995):

$$h_{ij} = \frac{h}{3}\delta_{ij} + \left(\partial_i\partial_j - \frac{\delta_{ij}}{3}\nabla^2\right)\mu + h_{ij}^V + h_{ij}^T\,.\qquad(3.18)$$

The vector part being constructed in terms of a divergenceless vector $h_i^V$

$$h_{ij}^V = \partial_i h_j^V + \partial_j h_i^V\,.\qquad(3.19)$$

The tensor part is traceless and transverse $(\partial_i h_j^{T\,i} = 0)$.

# 4   THE SCALAR CONTRIBUTION

We shall focus now on the magnetic scalar contribution to CMB anisotropies. The effect on metric perturbations is described by the Einstein equations with a source term given by the PMF EMT. We choose to work in the synchronous gauge where the scalar metric perturbation in the Fourier space is described by two scalar potentials, namely $h(k,\tau)$ and $\eta(k,\tau)$. The Einstein equations

with the contribution of PMF in the synchronous gauge are:

$$k^2\eta - \frac{1}{2}\mathcal{H}\dot{h} = -4\pi Ga^2(\Sigma_n\,\rho_n\delta_n + \rho_B)\,,$$

$$k^2\dot{\eta} = 4\pi Ga^2\Sigma_n(\rho_n + P_n)\theta_n\,,$$

$$\ddot{h} + 2\mathcal{H}\dot{h} - 2k^2\eta = -8\pi Ga^2(\Sigma_n\,c_{s\,n}^2\rho_n\delta_n$$

$$+\frac{\delta\rho_B}{3})\,,$$

$$\ddot{h} + 6\ddot{\eta} + 2\mathcal{H}(\dot{h} + 6\dot{\eta}) - 2k^2\eta = -24\pi Ga^2 \times$$

$$[\Sigma_n(\rho_n + P_n)\sigma_n + \sigma_B], \tag{4.20}$$

where $n$ represents the various species of the plasma, i.e. baryons, cold dark matter (CDM), photons and massless neutrinos. The conservation of the PMF EMT - $\nabla_\mu\tau_\nu^{\mu\,\mathrm{PMF}} = 0$ - implies that $\rho_B(\mathbf{x},\tau) = \rho_B(\mathbf{x},\tau_0)/a(\tau)^4$ and the following relation between the magnetic anisotropic stress $\sigma_B$, the magnetic energy density $\rho_B$ and the Lorentz force $L$ holds:

$$\sigma_B = \frac{\rho_B}{3} + L\,, \tag{4.21}$$

Such Lorentz force modifies the Euler equation for baryons velocity, leading to observational signatures (see FPP for the most recent discussion on this effect).

### 4.1 Initial Conditions

The magnetized adiabatic mode initial conditions in the synchronous gauge deep in the radiation era are:

$$h = C_1k^2\tau^2 - \frac{C_1(5+4R_\nu)}{36(15+4R_\nu)}k^4\tau^4$$

$$+\left[-\frac{55L_B}{336(15+4R_\nu)} + \frac{(-55+28R_\nu)\Omega_B}{1008(15+4R_\nu)}\right]k^4\tau^4$$

$$\eta = 2C_1 - \frac{5+4R_\nu}{6(15+4R_\nu)}C_1k^2\tau^2 +$$

$$\left[\frac{\Omega_B(-55+28R_\nu)}{168(15+4R_\nu)} - \frac{55L_B}{56(15+4R_\nu)}\right]k^2\tau^2$$

$$\delta_\gamma = -\Omega_B - \frac{2}{3}C_1k^2\tau^2 + \left[\frac{\Omega_B}{6} + \frac{L_B}{2(1-R_\nu)}\right]k^2\tau^2$$

$$\delta_\nu = -\Omega_B - \frac{2}{3}C_1k^2\tau^2 - \left[\frac{\Omega_B(1-R_\nu)}{6R_\nu} + \frac{L_B}{2R_\nu}\right]k^2\tau^2$$

$$\delta_b = -\frac{3}{4}\Omega_B - \frac{C_1}{2}k^2\tau^2 + \left[\frac{\Omega_B}{8} + \frac{3L_B}{8(1-R_\nu)}\right]k^2\tau^2$$

$$\delta_c = -\frac{3}{4}\Omega_B - \frac{C_1}{2}k^2\tau^2$$

$$\theta_\gamma = -\frac{C_1}{18}k^4\tau^3 - \left[\frac{\Omega_B}{4} + \frac{3}{4}\frac{L_B}{(1-R_\nu)}\right]k^2\tau$$

$$+\left[\frac{\Omega_B}{72} + \frac{L_B}{24(1-R_\nu)}\right]k^4\tau^3$$

$$\theta_b = \theta_\gamma$$

$$\theta_c = 0$$

$$\theta_\nu = -\frac{(23+4R_\nu)}{18(15+4R_\nu)}C_1k^4\tau^3$$

$$+\left[\frac{\Omega_B(1-R_\nu)}{4R_\nu} + \frac{3}{4}\frac{L_B}{R_\nu}\right]k^2\tau$$

$$-\left[\frac{(135+14R_\nu)L_B}{84R_\nu(15+4R_\nu)}\right.$$

$$\left.-\frac{(-270+161R_\nu+28R_\nu^2)\Omega_B}{504R_\nu(15+4R_\nu)}\right]k^4\tau^3$$

$$\sigma_\nu = \frac{4C_1}{3(15+4R_\nu)}k^2\tau^2 - \frac{\Omega_B}{4R_\nu} - \frac{3}{4}\frac{L_B}{R_\nu}$$

$$+\left[\frac{-\Omega_B(-55+28R_\nu)}{56R_\nu(15+4R_\nu)} + \frac{165L_B}{56R_\nu(15+4R_\nu)}\right]k^2\tau^2$$

$$F_{3\nu} = -\frac{6}{7}\left[\frac{\Omega_B}{4R_\nu} + \frac{3}{4}\frac{L_B}{R_\nu}\right]k\tau\,, \tag{4.22}$$

where $\Omega_B = \rho_B/(\rho_\nu + \rho_\gamma)$, $L_B = L/(\rho_\nu + \rho_\gamma)$, $R_\nu = \rho_\nu/(\rho_\nu + \rho_\gamma)$, $C_1$ is the constant which characterizes the regular growing adiabatic mode as given in Ma and Bertschinger (1995). The result reported is different from the one reported in FPP because we are adding the first non-trivial terms in $\mathcal{O}(\Omega_B, L_B)$ for $h, \delta_c$ and because of a different truncation in the neutrino hierarchy. The term $\mathcal{O}(k^4\tau^4)$ in $h$ (which also contains the next-to-leading term of the adiabatic mode) has been obtained by taking self-consistently the required order in all the variables in Eqs. (4.22). For simplicity we have written the $\mathcal{O}(k^4\tau^4)$ term only in $h$ (since it is the leading term for the magnetic solution) and omitted these higher order terms in all the other variables. Here we also choose to truncate the hierarchy at $F_{4\nu} = 0$ instead of $F_{3\nu} = 0$ as in FPP. This change affects the magnetic next to leading order terms in the velocity and anisotropic stress of neutrinos and in the metric perturbation $\eta$. The equation for the evolution of the $F_{3\nu}$ is:

$$\dot{F}_{3\nu} = \frac{6}{7}k\sigma_\nu\,, \tag{4.23}$$

while the neutrino anisotropic stress equation becomes:

$$2\dot{\sigma}_\nu = \frac{8}{15}\theta_\nu - \frac{3}{5}kF_{3\nu} + \frac{4}{15}\dot{h} + \frac{8}{5}\dot{\eta}\,. \tag{4.24}$$

Note how the presence of a SB of PMFs induces a new independent mode in matter and metric perturbations, i.e. the fully magnetic mode obtained by setting $C_1 = 0$ in Eq. (4.22). This new independent mode is the particular solution of the inhomogeneous system of the Einstein-Botzmann differential equations: the SB of PMF treated as a stiff source acts indeed as a force term in the system of linear differential equations. Whereas the sum of the fully magnetic mode with the curvature one can be with any correlation as for an isocurvature mode, the nature of the fully magnetic mode - and therefore its effect - is different: the isocurvature modes are solutions of the homogeneous system (in which all the species have both background and perturbations),

whereas the fully magnetic one is the solution of the inhomogeneous system sourced by a fully inhomogeneous component.

It is interesting to note how the magnetic contribution drops from the metric perturbation at leading order, although is larger than the adiabatic solution for photons, neutrinos and baryons. This is due to a compensation which nullifies the sum of the leading contributions (in the long-wavelength expansion) in the single species energy densities and therefore in the metric perturbations. A similar compensation exists for a network of topological defects, which does not carry a background energy-momentum tensor as the PMF SB studied here[4].

## 4.2 Analytic Description of the Scalar Magnetic Contribution on Large Angular Scales

In this subsection we give an analytic description for the scalar magnetic contribution to CMB anisotropies on large angular scales given by the initial conditions in Eq. (4.22) and computed by our modified version of CAMB. The Sachs-Wolfe term is $\delta T/T_{|\rm SW} \sim \delta_r/4 + \psi$, where $\delta_r$ is the radiation density contrast and $\psi$ is one of the metric potentials in the longitudinal gauge:

$$ds^2 = a^2(\eta) \left[ -(1+2\psi)d\eta^2 + (1-2\phi)\gamma_{ij}dx^i dx^j \right] \quad (4.25)$$

For adiabatic initial conditions is simply $\delta T/T_{|\rm SW} \sim \psi/3$ since $\delta_r \simeq -8\psi/3$ in the matter dominated era on large scales.

The Sachs-Wolfe term for the scalar magnetic mode generated by a SB of PMF can be obtained by using the initial conditions given in the synchronous gauge in Eq. (4.22). By making a gauge transformation, we obtain at leading order in the radiation era:

$$\begin{aligned} \frac{\delta_r}{4} &\simeq& -\frac{\Omega_B}{4} + \frac{\Omega_B(1-R_\nu)+3L_B}{15+4R_\nu} \\ \psi &\simeq& -\frac{\Omega_B(55-28R_\nu)+165L_B}{14(15+4R_\nu)} \,. \end{aligned} \quad (4.26)$$

In the radiation era, because of compensation, the metric potential are just proportional to $\Omega_B$ and not to $\Omega_B/k^2$ as obtained by Kahniashvili and Ratra (2006). As we will show in the following, the same holds in the matter era.

Now let us assume that in the matter era:

$$\frac{\delta T}{T}_{|\rm SW} = \alpha \frac{\Omega_B}{4} \quad (4.27)$$

and we compute the scalar contribution to CMB anisotropies for $n > -3/2$ by solving the integral:

---

[4] Note however that a network of topological defects does not scale with radiation and interacts only gravitationally with the rest of matter, i.e. a Lorentz term is absent.

$$C_\ell^{S,magnetic} \simeq \frac{\alpha^2}{8\pi} \int_0^{k_D} dk k^2 |\Omega_B|^2 j_\ell^2(k\eta_0) \,, \quad (4.28)$$

where we have insterted an upper cut-off $k_D$ in order to use the infrared expansion of $|\rho_B(k)|$, obtained in FPP:

$$|\rho_B(k)|^2 \simeq \frac{A^2 k_D^{2n+3}}{128\pi^4 k_*^{2n}(3+2n_B)} \,. \quad (4.29)$$

By using the result (Abramowitz and Stegun 1965)

$$\int_0^y dx x J_{\ell+1/2}^2(x) = \frac{y^2}{2} \left[ J_{\ell+1/2}^2(y) - J_{\ell-1/2}(y)J_{\ell+3/2}(y) \right] \,,$$

we obtain for $n > -3/2$ and $y >> 1$:

$$C_\ell^{S,magnetic} \simeq \frac{\alpha^2(n+3)^2 \langle B^2 \rangle^2}{512\pi(2n+3)\rho_{REL,0}^2 k_D^2 \eta_0^2} \,. \quad (4.30)$$

The scalar magnetic contribution to CMB anisotropies on large angular scales is therefore white noise ($C_\ell^{S,magnetic} \propto \ell^2$) for $\ell < 400$ and $n_B > -3/2$; the slope in $\ell$ of Eq. (4.30) and of the numerical results obtained with our modified version of CAMB agree very well. By using an analogous procedure for $n_B = -5/2$, we obtain analitically $C_\ell^{S,magnetic} \sim 1/\ell$ to be compared with the numerical results -$\sim 1/\ell^{0.4}$- obtained with our modified version of CAMB. The $\alpha$ parameter in Eq. (4.30) we can fit from our numerical results inherits a dependence on $n_B$, $k_D$ and is tipically $\sim \mathcal{O}(0.01-0.1)$.

## 5 THE VECTOR CONTRIBUTION

In this section we shall review the evolution of vector perturbations induced by a SB of PMF as treated in Lewis (2004). The vector metric perturbation is described through a divergenceless vector:

$$h_{ij}^V = \partial_i h_j + \partial_j h_i \quad (5.31)$$

where we have

$$\partial_i h_i = 0 \quad (5.32)$$

The divergenceless condition assures that vector mode does not support density perturbations. The Einstein equations in the presence of PMF for the vector metric perturbations simply reduce to:

$$\dot{h}^V + 2\mathcal{H}h^V = -16\pi G a^2 (\Pi_\nu^{(V)} + \Pi_\gamma^{(V)} + \Pi_B^{(V)})/k \quad (5.33)$$

Conservation equations for PMF also in the vector case reduce to a relation between isotropic and anisotropic pressure and the vector Lorentz force:

$$-\nabla_i p^B + \nabla_j \Pi_{ij}^{(V)B} = L_i^B \quad (5.34)$$

The Lorentz force induced on baryons, in analogy with what we found for the scalar case, modifies the baryon vector velocity equation:

$$\dot{v}_b + \mathcal{H}v_b = -\frac{\rho_\gamma}{\rho_b} \left( \frac{4}{3} n_e a\sigma_T(v_b - v_\gamma) - \frac{L^V}{\rho_\gamma} \right) \quad (5.35)$$

where we have neglected the baryon homogeneous pressure ($p_b/\rho_b << 1$). In order to investigate the effect of magnetized vector perturbations it is necessary to calculate the Fourier spectra for the vector projection of the PMF EMT and the Lorentz force. Since these two quantities are related by:

$$L_i^{(V)} = k\Pi_i^{(V)} \,, \tag{5.36}$$

we need only one spectrum to compute for the vector part, as for the tensor part described in the next section and differently from the scalar part.

## 6  THE TENSOR CONTRIBUTION

Inflationary tensor modes, namely primordial gravitational waves, are a key prediction of the standard inflationary model, and therefore their indirect observation through CMB anisotropies is one of the crucial point of modern cosmology. However PMF carrying anisotropic stress are themselves a source of tensor perturbations. Therefore the presence of PMF affects inflationary tensor modes and creates a new independent fully magnetic tensor mode in analogy to what we found for scalar perturbations. The evolution equation for the metric tensor perturbation $h_{ij}$ is:

$$\ddot{h}_{ij} + 2\mathcal{H}\dot{h}_{ij} + k^2 h_{ij} = 16\pi G a^2 (\rho_\nu \pi_{ij}^\nu + \Pi_{ij}^{(B,T)}) \,. \tag{6.37}$$

which, for each polarization state deep in radiation era reads

$$\ddot{h}_k^T + \frac{2}{\tau}\dot{h}_k^T + k^2 h_k^T = \frac{6}{\tau^2}[R_\nu \sigma_\nu^{(T)} + (1 - R_\nu)\tilde{\Pi}_B^{(T)}] \tag{6.38}$$

where $\tilde{\Pi}_B^{(T)}$ represents the time independent variable $\Pi_B^{(T)}/\rho_\gamma$. The large scales solution to this equation can be found expanding $h_k$ in powers of $(k\tau)$. In order to keep the leading and the next-to-leading terms we need to take into account the neutrino octopole ($J_3$), truncating the propagation of anisotropic stress through higher moments by posing $J_4 = 0$. Hence the neutrino anisotropic stress evolves according to

$$\dot{\sigma}_\nu^{(T)} = -\frac{4}{15}\dot{h}_k - \frac{k}{3}J_3$$
$$\dot{J}_3 = \frac{3}{7}k\sigma_\nu^{(T)} \tag{6.39}$$

and the solution is then:

$$h_k = A\left[1 - \frac{5(k\tau)^2}{2(15 + 4R_\nu)}\right] + \frac{15(1 - R_\nu)\tilde{\Pi}_B^{(T)}(k\tau)^2}{14(15 + 4R_\nu)} \,,$$
$$\sigma_\nu^{(T)} = -\frac{(1 - R_\nu)}{R_\nu}\tilde{\Pi}_B^{(T)}\left[1 - \frac{15(k\tau)^2}{14(15 + 4R_\nu)}\right]$$
$$+ A\frac{2(k\tau)^2}{3(15 + 4R_\nu)} \,. \tag{6.40}$$

The presence of magnetic fields is responsible for the new leading term in $\sigma_\nu^{(T)}$ - otherwise absent. This is the so-called compensation between collisionless fluid and magnetic anisotropic stresses due to fact that magnetic fields gravitate only at perturbative level.

Note that the compensation between anisotropic stresses turns on only after neutrino decoupling, an epoch which is much earlier than the usual initial time at which cosmological perturbations are evolved in an Einstein-Boltzmann code. The detailed study of the evolution of gravitational waves during neutrino decoupling is an interesting issue, but clearly beyond the purpose of the present project.

## 7  RESULTS FOR CMB ANISOTROPIES

In this section we now present the temperature and polarization CMB spectra including the full contribution of SB of PMF. In addition to the $C_\ell$ obtained by the adiabatic mode in absence of primordial magnetic fields, we add the three contributions $C_\ell^{\mathrm{S,V,T}}$ described in Sects. 4,5,6, i.e. scalar, vector, tensor, respectively, computed separately by our modified version of CAMB. In Fig.3 and Fig.4 we show the results for $n_B = 2$ and $-5/2$, respectively. For the initial conditions of the scalar magnetic mode, we use as initial conditions Eq. (4.22) with $C_1 = 0$; for those of the tensor mode the ones in Eq. (6.40) with $A = 0$. For the initial conditions for the vector mode we use the ones already implemented in CAMB, described in Lewis (2004). All the formulae for magnetic spectra needed - $\Omega_B$, $L_B$, $\Pi_V$, $\Pi_T$ - are given in our appendices; the signs of $L_B$ and $\Omega_B$ are taken as opposite, as explained in FPP.

For all the values of $n_B$ considered here, the CMB temperature pattern generated by the SB of PMF is dominated by the scalar contribution at low and intermediate multipoles; the vector contribution takes over the scalar one at high multipoles, whereas the tensor one is always subleading with respect to scalar and vector.

It is interesting to note that the $B$ polarization signal due to the vector contribution is always larger than the tensor one. The $B$ mode produced by vector perturbations has a power spectrum which can be steeper than the one produced by lensing with a peak around $\ell \sim \text{few} \times 10^3$; therefore, for suitable values of the magnetic field amplitude the $B$ mode produced by a SB of PMF can be larger than the lensing one for any $n_B$. Fig. 5 shows how the vector contribution to the $B$ spectrum depends on $n_B$. For $n_B > -3/2$ the $B$ spectra from the vector contribution are almost indistinguishable for different $n_B$, because $\Pi_B^{(V)}$ is white noise for $k \ll k_D$; for $-3 < n_B \leq -3/2$ we note a dependence of the $B$ spectrum on $n_B$. Analogous dependence on $n_B$ also holds for the vector contribution to $TT$.
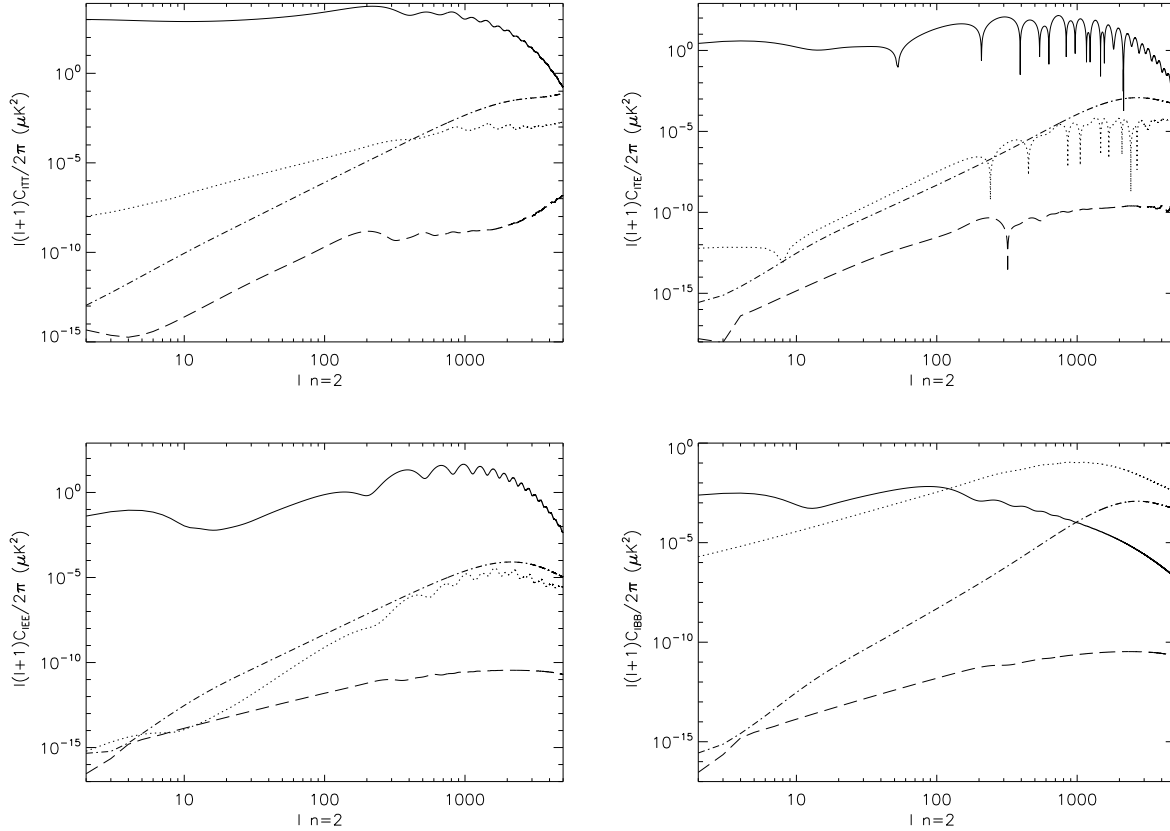
**Figure 3.** CMB anisotropies angular power spectrum for temperature (TT hereafter, top-left panel), temperature-E polarization cross correlation (TE hereafter, top-right panel), E polarization (EE hereafter, bottom-left panel), B polarization (BB hereafter, bottom-right panel). The solid line is the adiabatic scalar contribution in TT, TE, EE panels, whereas it is the tensor homogeneous contribution in the BB panel (for a tensor-to-scalar ratio $r = 0.1$); the dotted, dot-dashed, dashed are the scalar, vector and tensor contributions of a SB of PMF respectively for $\sqrt{\langle B^2 \rangle} = 7.5$ nG, $n_B = 2$ and $k_D = 2\pi \, \mathrm{Mpc}^{-1}$. The dotted line in the BB panel is the lensing contribution. The cosmological parameters of the flat $\Lambda CDM$ model are $\Omega_b \, h^2 = 0.022$, $\Omega_c \, h^2 = 0.123$, $z_{\mathrm{re}} = 12$, $n_s = 1$, $H_0 = 100 \, h \, \mathrm{km \, s^{-1} \, Mpc^{-1}} = 72 \, \mathrm{km \, s^{-1} \, Mpc^{-1}}$.

## 8    CONCLUSION

We have obtained the Fourier spectra of the relevant scalar, vector and tensor energy-momentum components of the SB of PMF extending the method used in FPP only for the scalar. As already discussed for the scalar sector in FPP, we have shown how the correct evaluation of the convolution integrals leads to differences in the vector and tensor parts of the PMF Fourier spectrum previously found in Mack, Kahniashvili and Kosowsky (2002).

We have then shown the comparison of the scalar, vector and tensor contributions to CMB anisotropies of the new inhomogeneous modes generated by the SB of PMF, by using the correct convolutions for the energy-momentum tensor of the PMF SB. We have shown that the dominant contributions are from scalar and vector perturbations, respectively for low and high $\ell$. We have

given an analytic description of the Sachs-Wolfe contribution of the scalar mode, which agrees very well with the numerical result of our modified version of CAMB (Lewis,Challinor and Lasenbly 2000) and takes into account the compensation effect on large scales which is generic when a fully inhomogeneous source is present. The slope in $\ell$ of the vector power spectrum we obtain numerically agrees very well with previous analytic (Mack, Kahniashvili and Kosowsky 2002) and numerical (Lewis 2004) results. As already found in (Lewis 2004), the $B$ signal by vector perturbations, with a peak slightly dependent on $n_B$ around $\ell \sim 2000$, has a shape different either from the inflationary gravitational waves or the lensing signal. We have characterized its dependence on $n_B$ and shown how this is non trivial for $n_B \leq -3/2$: such signal can be constrained by Planck ([Planck Collaboration] 2006) and future small scale CMB polarization experiments.
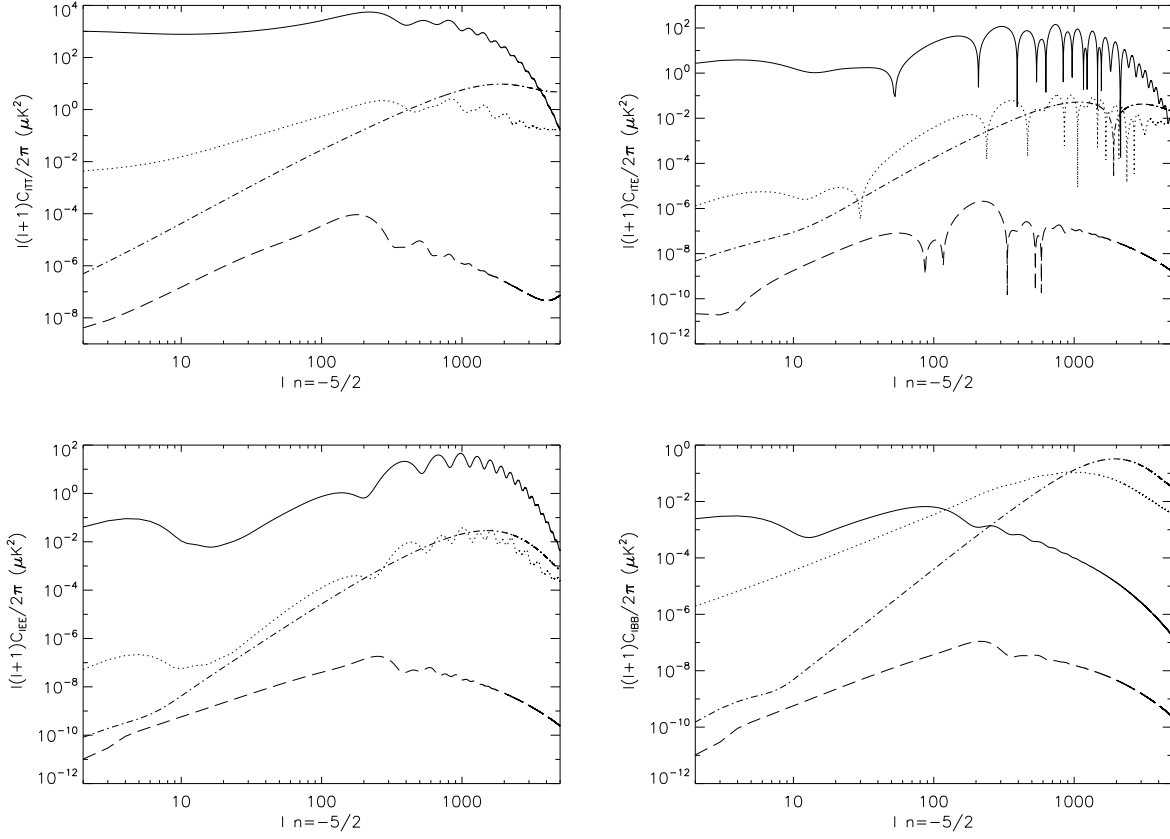
**Figure 4.** CMB angular power spectrum for TT (left top panel), TE (left top panel), EE (bottom left), BB (bottom right). The solid line is the adiabatic scalar contribution in TT, TE, EE panels, whereas it is the tensor homogeneous contribution in the BB panel (for a tensor-to-scalar ratio $r = 0.1$); the dotted, dot-dashed, dashed are the scalar, vector and tensor contributions of a SB of PMF respectively for $\sqrt{\langle B^2 \rangle} = 7.5$ nG, $n_B = -5/2$ and $k_D = 2\pi\,\mathrm{Mpc}^{-1}$. The dotted line in the BB panel is the lensing contribution. The cosmological parameters of the flat $\Lambda CDM$ model are the same as in Fig. 3.
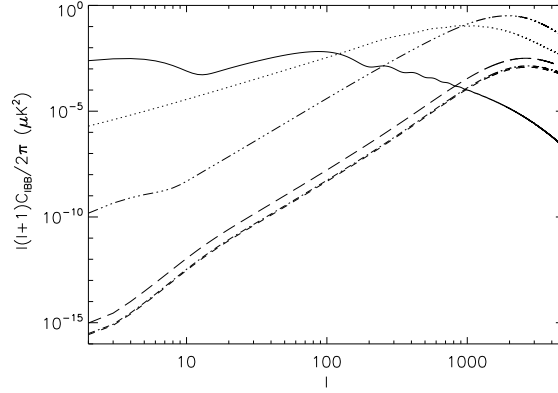
**Figure 5.** Vector contributions to the CMB angular power spectrum for BB. The solid line is the tensor homogeneous contribution for a tensor-to-scalar ratio $r = 0.1$ and the dotted line is the lensing contribution with cosmological parameters as in the previous figures; the triple-dotted, long dashed, dot-dashed and dashed are the vector spectra obtained with $\sqrt{\langle B^2 \rangle} = 7.5$ nG, $k_D = 2\pi \mathrm{Mpc}^{-1}$, for $n_B = -2.5, -1.5, -1, 2$, respectively. Note how the spectra for $n_B = -1$ and $n_B = 2$ are super-imposed since the Fourier spectra of the vector part of the PMF EMT are both white noise for $k \ll k_D$ for these spectral indexes.

## APPENDIX A: EMT FOURIER SPECTRA

We use the convolutions for the PMF EMT spectra with the parametrization for the magnetic field power spectrum given in Eq. (2.5). Since $P_B(k) = 0$ for $k > k_D$, two conditions need to be taken into account:

$$p < k_D \,, \qquad\qquad |\mathbf{k} - \mathbf{p}| < k_D \,. \qquad\qquad (A1)$$

The second condition introduces a $k$-dependence on the angular integration domain and the two allow the energy power spectrum to be non zero only for $0 < k < 2k_D$. Such conditions split the double integral (over $\gamma$ and over $p$) in three parts depending on the $\gamma$ and $p$ lower and upper limit of integration. For simplicity we normalize the Fourier wavenumber to $k_D$ and we show the integrals with this convention. A sketch of the integration is thus the following:

1)    $0 < k < 1$

$$\int_0^{1-k} dp \int_{-1}^1 d\gamma \,\ldots + \int_{1-k}^1 dp \int_{\frac{k^2+p^2-1}{2kp}}^1 d\gamma \,\ldots \equiv \int_0^{1-k} dp I_a(p,k) + \int_{1-k}^1 dp I_b(p,k)$$

2)    $1 < k < 2$

$$\int_{k-1}^1 dp \int_{\frac{k^2+p^2-1}{2kp}}^1 d\gamma \,\ldots \equiv \int_{k-1}^1 dp I_c(p,k) \qquad\qquad (A2)$$

Particular care must be used in the radial integrals. In particular, the presence of the term $|k - p|^{n+2}$ in both

integrands, needs a further splitting of the integral domain for odd $n$:

$$\int_0^{(1-k)} dp \rightarrow \begin{cases} k < 1/2 \begin{cases} \int_0^k dp... & \text{with} \quad p < k \\ \int_k^{(1-k)} dp... & \text{with} \quad p > k \end{cases} \\ k > 1/2 \quad \int_0^{(1-k)} dp... & \text{with} \quad p < k \end{cases}$$

$$\int_{(1-k)}^1 dp \rightarrow \begin{cases} k < 1/2 \quad \int_{(1-k)}^1 dp... & \text{with} \quad p > k \\ k > 1/2 \begin{cases} \int_{(1-k)}^k dp... & \text{with} \quad p < k \\ \int_k^1 dp... & \text{with} \quad p > k \end{cases} \end{cases}$$

$$\int_{(k-1)}^1 dp \rightarrow \begin{cases} 1 < k < 2 \quad \int_{(k-1)}^1 dp... & \text{with} \quad p < k \end{cases}$$

Following the scheme (A2) we can now perform the integration over $p$. Our exact results are given for particular values of $n_B$.

**A1** $\quad n_B = 3$

$$|\rho_B(k)|^2_{n_B=3} = \frac{A^2 k_D^9}{512\pi^4 k_*^6} \begin{cases} \frac{4}{9} - \tilde{k} + \frac{20\tilde{k}^2}{21} - \frac{5\tilde{k}^3}{12} + \frac{4\tilde{k}^4}{75} + \frac{4\tilde{k}^6}{315} - \frac{\tilde{k}^9}{1575} & \text{for} \quad 0 \le \tilde{k} \le 1 \\ -\frac{4}{9} - \frac{88}{525\tilde{k}} + \frac{13\tilde{k}}{15} - \frac{20\tilde{k}^2}{21} + \frac{17\tilde{k}^3}{36} - \frac{4\tilde{k}^4}{75} - \frac{4\tilde{k}^6}{315} + \frac{\tilde{k}^9}{525} & \text{for} \quad 1 \le \tilde{k} \le 2 \end{cases},$$

$$|\Pi_B^{(V)}(k)|^2_{n_B=3} = \frac{A^2 k_D^9}{256\pi^4 k_*^6} \begin{cases} \frac{28}{135} - \frac{5\tilde{k}}{12} + \frac{296\tilde{k}^2}{735} - \frac{2\tilde{k}^3}{9} + \frac{92\tilde{k}^4}{1575} - \frac{32\tilde{k}^6}{10395} + \frac{2\tilde{k}^9}{11025} & \text{for} \quad 0 \le \tilde{k} \le 1 \\ -\frac{28}{135} - \frac{32}{24255\tilde{k}^5} + \frac{4}{945\tilde{k}^3} + \frac{44}{525\tilde{k}} + \frac{23\tilde{k}}{60} - \frac{296\tilde{k}^2}{735} + \frac{2\tilde{k}^3}{9} - \frac{92\tilde{k}^4}{1575} + \frac{32\tilde{k}^6}{10395} - \frac{2\tilde{k}^9}{33075} & \text{for} \quad 1 \le \tilde{k} \le 2 \end{cases},$$

$$|\Pi_B^{(T)}(k)|^2_{n_B=3} = \frac{A^2 k_D^9}{256\pi^4 k_*^6} \begin{cases} \frac{56}{135} - \frac{7\tilde{k}}{6} + \frac{1112\tilde{k}^2}{735} - \frac{127\tilde{k}^3}{144} + \frac{296\tilde{k}^4}{1575} + \frac{104\tilde{k}^6}{10395} - \frac{29\tilde{k}^9}{11025} & \text{for} \quad 0 \le \tilde{k} \le 1 \\ -\frac{56}{135} + \frac{16}{24255\tilde{k}^5} + \frac{8}{945\tilde{k}^3} + \frac{32}{525\tilde{k}} + \frac{37\tilde{k}}{30} - \frac{1112\tilde{k}^2}{735} + \frac{43\tilde{k}^3}{48} - \frac{296\tilde{k}^4}{1575} - \frac{104\tilde{k}^6}{10395} + \frac{29\tilde{k}^9}{33075} & \text{for} \quad 1 \le \tilde{k} \le 2 \end{cases}.$$

**A2** $\quad n_B = 2$

$$|\rho_B(k)|^2_{n_B=2} = \frac{A^2 k_D^7}{512\pi^4 k_*^4} \left[ \frac{4}{7} - \tilde{k} + \frac{8\tilde{k}^2}{15} - \frac{\tilde{k}^5}{24} + \frac{11\tilde{k}^7}{2240} \right],$$

$$|\Pi_B^{(V)}(k)|^2_{n_B=2} = \frac{A^2 k_D^7}{256\pi^4 k_*^4} \left[ \frac{4}{15} - \frac{5\tilde{k}}{12} + \frac{4\tilde{k}^2}{15} - \frac{\tilde{k}^3}{12} + \frac{7\tilde{k}^5}{960} - \frac{\tilde{k}^7}{1920} \right],$$

$$|\Pi_B^{(T)}(k)|^2_{n_B=2} = \frac{A^2 k_D^7}{256\pi^4 k_*^4} \left[ \frac{8}{15} - \frac{7\tilde{k}}{6} + \frac{16\tilde{k}^2}{15} - \frac{7\tilde{k}^3}{24} - \frac{13\tilde{k}^5}{480} + \frac{11\tilde{k}^7}{1920} \right].$$

**A3** $\quad n_B = 1$

$$|\rho_B(k)|^2_{n_B=1} = \frac{A^2 k_D^5}{512\pi^4 k_*^2} \begin{cases} \frac{4}{5} - \tilde{k} + \frac{\tilde{k}^3}{4} - \frac{4}{15}\tilde{k}^4 - \frac{\tilde{k}^5}{5} & \text{for} \quad 0 \le \tilde{k} \le 1 \\ \frac{8}{15\tilde{k}} - \frac{4}{5} + \frac{\tilde{k}}{3} + \frac{\tilde{k}^3}{4} - \frac{4\tilde{k}^4}{15} + \frac{\tilde{k}^5}{15} & \text{for} \quad 1 \le \tilde{k} \le 2 \end{cases},$$

$$|\Pi_B^{(V)}(k)|^2_{n_B=1} = \frac{A^2 k_D^5}{256\pi^4 k_*^2} \begin{cases} \frac{28}{75} - \frac{5\tilde{k}}{12} + \frac{4\tilde{k}^2}{35} - \frac{8\tilde{k}^4}{315} + \frac{\tilde{k}^5}{50} & \text{for} \quad 0 \le \tilde{k} \le 1 \\ -\frac{32}{1575\tilde{k}^5} + \frac{4}{105\tilde{k}^3} + \frac{4}{15\tilde{k}} - \frac{28}{75} + \frac{\tilde{k}}{4} - \frac{4\tilde{k}^2}{35} + \frac{8\tilde{k}^4}{315} - \frac{\tilde{k}^5}{150} & \text{for} \quad 1 \le \tilde{k} \le 2 \end{cases},$$

$$|\Pi_B^{(T)}(k)|^2_{n_B=1} = \frac{A^2 k_D^5}{256\pi^4 k_*^2} \begin{cases} \frac{56}{75} - \frac{7\tilde{k}}{6} + \frac{64\tilde{k}^2}{105} - \frac{\tilde{k}^3}{16} + \frac{8\tilde{k}^4}{63} - \frac{4\tilde{k}^5}{25} & \text{for} \quad 0 \le \tilde{k} \le 1 \\ \frac{16}{1575\tilde{k}^5} + \frac{8}{105\tilde{k}^3} - \frac{56}{75} + \frac{3\tilde{k}}{2} - \frac{64\tilde{k}^2}{105} + \frac{\tilde{k}^3}{16} - \frac{8\tilde{k}^4}{63} - \frac{4\tilde{k}^5}{75} & \text{for} \quad 1 \le \tilde{k} \le 2 \end{cases}.$$

**A4** $n_B = 0$

$$|\rho_B(k)|^2_{n_B=0} = \frac{A^2 k_D^3}{512\pi^4}\left[\frac{29}{24} - \frac{17\tilde{k}}{16} - \frac{7\tilde{k}^2}{8} + \frac{53\tilde{k}^3}{96} + \frac{\pi^2\tilde{k}^3}{24} - \frac{\log|1-\tilde{k}|}{8\tilde{k}} + \frac{\tilde{k}\log|1-\tilde{k}|}{2} - \frac{3\tilde{k}^3\log|1-\tilde{k}|}{8}\right.$$
$$\left. + \frac{\tilde{k}^3\log|1-\tilde{k}|\log\tilde{k}}{2} - \frac{\tilde{k}^3\log^2\tilde{k}}{4} - \frac{\tilde{k}^3\text{PolyLog}[2,\frac{-1+\tilde{k}}{\tilde{k}}]}{2}\right],$$

$$|\Pi_B^{(V)}(k)|^2_{n_B=0} = \frac{A^2 k_D^3}{256\pi^4}\left[\frac{53}{96} + \frac{1}{32\tilde{k}^4} + \frac{1}{64\tilde{k}} - \frac{1}{32\tilde{k}^2} - \frac{5}{384\tilde{k}} - \frac{29\tilde{k}}{64} - \frac{5\tilde{k}^2}{96} + \frac{55\tilde{k}^3}{768} + \frac{\log|1-\tilde{k}|}{32\tilde{k}^5} - \frac{\log|1-\tilde{k}|}{24\tilde{k}^3}\right.$$
$$\left. - \frac{\log|1-\tilde{k}|}{16\tilde{k}} + \frac{\tilde{k}\log|1-\tilde{k}|}{8} - \frac{5\tilde{k}\log|1-\tilde{k}|}{96}\right],$$

$$|\Pi_B^{(T)}(k)|^2_{n_B=0} = \frac{A^2 k_D^3}{256\pi^4}\left[\frac{293}{192} - \frac{1}{64\tilde{k}^4} - \frac{1}{128\tilde{k}} - \frac{17}{192\tilde{k}^2} - \frac{35}{768\tilde{k}} - \frac{397\tilde{k}}{384} - \frac{17\tilde{k}^2}{192} + \frac{181\tilde{k}^3}{1536} + \frac{\pi^2\tilde{k}^3}{96} - \frac{\log|1-\tilde{k}|}{64\tilde{k}^5} - \frac{\log|1-\tilde{k}|}{12\tilde{k}^3}\right.$$
$$\left. + \frac{5\log|1-\tilde{k}|}{16\tilde{k}} - \frac{\tilde{k}\log|1-\tilde{k}|}{4} + \frac{7\tilde{k}^3\log|1-\tilde{k}|}{192} + \frac{\tilde{k}^3\log|1-\tilde{k}|\log\tilde{k}}{8} - \frac{\tilde{k}^3\log^2\tilde{k}}{16} - \frac{\tilde{k}^3\text{PolyLog}[2\frac{-1+\tilde{k}}{\tilde{k}}]}{8}\right].$$

**A5** $n_B = -1$

$$|\rho_B(k)|^2_{n_B=-1} = \frac{A^2 k_D k_*^2}{512\pi^4}\begin{cases} 4 - 5\tilde{k} + \frac{4\tilde{k}^2}{3} + \frac{\tilde{k}^3}{4} & \text{for} \quad 0 \leq \tilde{k} \leq 1 \\ -4 + \frac{8}{3\tilde{k}} + 3\tilde{k} - \frac{4\tilde{k}^2}{3} + \frac{\tilde{k}^3}{4} & \text{for} \quad 1 \leq \tilde{k} \leq 2 \end{cases},$$

$$|\Pi_B^{(V)}(k)|^2_{n_B=-1} = \frac{A^2 k_D k_*^2}{256\pi^4}\begin{cases} \frac{28}{15} - \frac{7\tilde{k}}{4} + \frac{16\tilde{k}^2}{105} & \text{for} \quad 0 \leq \tilde{k} \leq 1 \\ -\frac{28}{15} + \frac{32}{105\tilde{k}^5} - \frac{4}{15\tilde{k}^3} + \frac{4}{3\tilde{k}} + \frac{11\tilde{k}}{12} - \frac{16\tilde{k}^2}{105} & \text{for} \quad 1 \leq \tilde{k} \leq 2 \end{cases},$$

$$|\Pi_B^{(T)}(k)|^2_{n_B=-1} = \frac{A^2 k_D k_*^2}{256\pi^4}\begin{cases} \frac{56}{15} - \frac{5\tilde{k}}{2} - \frac{8\tilde{k}^2}{105} + \frac{\tilde{k}^3}{16} & \text{for} \quad 0 \leq \tilde{k} \leq 1 \\ -\frac{56}{15} - \frac{16}{105\tilde{k}^5} - \frac{8}{15\tilde{k}^3} + \frac{16}{3\tilde{k}} + \frac{\tilde{k}}{6} + \frac{8\tilde{k}^2}{105} + \frac{\tilde{k}^3}{16} & \text{for} \quad 1 \leq \tilde{k} \leq 2 \end{cases}.$$

**A6** $n_B = -3/2$

$$|\rho_B(k)|^2_{n_B=-3/2} = \frac{A^2 k_*^3}{512\pi^4}\begin{cases} \frac{232}{45\sqrt{1-\tilde{k}}} + \frac{88}{15\tilde{k}} - \frac{88}{15\sqrt{1-\tilde{k}}\tilde{k}} - 2\pi + \frac{4\tilde{k}}{3} - \frac{32\tilde{k}}{45\sqrt{1-\tilde{k}}} + \frac{64\tilde{k}^2}{45\sqrt{1-\tilde{k}}} \\ + \frac{\tilde{k}^3}{9} + 8\log[1 + \sqrt{1-\tilde{k}}] - 4\log\tilde{k} & \text{for} \quad 0 \leq \tilde{k} \leq 1 \\ -\frac{232}{45\sqrt{-1+\tilde{k}}} + \frac{88}{15\tilde{k}} + \frac{88}{15\sqrt{-1+\tilde{k}}\tilde{k}} + \frac{4\tilde{k}}{3} + \frac{32\tilde{k}}{45\sqrt{-1+\tilde{k}}} - \frac{64\tilde{k}^2}{45\sqrt{-1+\tilde{k}}} \\ + \frac{\tilde{k}^3}{9} - 4\arctan\left[\frac{1}{\sqrt{-1+\tilde{k}}}\right] + 4\arctan\left[\sqrt{-1+\tilde{k}}\right] & \text{for} \quad 1 \leq \tilde{k} \leq 2 \end{cases},$$

$$|\Pi_B^{(V)}(k)|^2_{n_B=-3/2} = \frac{A^2 k_*^3}{256\pi^4}\begin{cases} \frac{4936}{1755\sqrt{1-\tilde{k}}} + \frac{1024}{2925\tilde{k}^5} - \frac{1024}{2925\sqrt{1-\tilde{k}}\tilde{k}^5} - \frac{14\pi}{15} + \frac{512}{2925\sqrt{1-\tilde{k}}\tilde{k}^4} \\ - \frac{32}{135\tilde{k}^3} + \frac{2464}{8775\sqrt{1-\tilde{k}}\tilde{k}^3} - \frac{848}{8775\sqrt{1-\tilde{k}}\tilde{k}^2} + \frac{44}{15\tilde{k}} - \frac{5176}{1755\sqrt{1-\tilde{k}}\tilde{k}} + \frac{\tilde{k}}{3} \\ - \frac{224\tilde{k}}{1755\sqrt{1-\tilde{k}}} + \frac{448\tilde{k}^2}{1755\sqrt{1-\tilde{k}}} + \frac{56\log[1+\sqrt{1-\tilde{k}}]}{15} - \frac{28\log\tilde{k}}{15} & \text{for} \quad 0 \leq \tilde{k} \leq 1 \\ -\frac{4936}{1755\sqrt{-1+\tilde{k}}} + \frac{1024}{2925\tilde{k}^5} + \frac{1024}{2925\sqrt{-1+\tilde{k}}\tilde{k}^5} - \frac{512}{2925\sqrt{-1+\tilde{k}}\tilde{k}^4} \\ - \frac{32}{135\tilde{k}^3} - \frac{2464}{8775\sqrt{-1+\tilde{k}}\tilde{k}^3} + \frac{848}{8775\sqrt{-1+\tilde{k}}\tilde{k}^2} + \frac{44}{15\tilde{k}} + \frac{5176}{1755\sqrt{-1+\tilde{k}}\tilde{k}} + \frac{\tilde{k}}{3} \\ + \frac{224\tilde{k}}{1755\sqrt{-1+\tilde{k}}} - \frac{448\tilde{k}^2}{1755\sqrt{-1+\tilde{k}}} - \frac{28\arctan\left[\frac{1}{\sqrt{-1+\tilde{k}}}\right]}{15} + \frac{28\arctan\left[\sqrt{-1+\tilde{k}}\right]}{15} & \text{for} \quad 1 \leq \tilde{k} \leq 2 \end{cases},$$

$$
|\Pi_B^{(T)}(k)|^2_{n_B=-3/2} = \frac{A^2 k_*^3}{256\pi^4}
\begin{cases}
\begin{aligned}
& \frac{16304}{1755\sqrt{1-\tilde{k}}} - \frac{512}{2925\tilde{k}^5} + \frac{512}{2925\sqrt{1-\tilde{k}}\tilde{k}^5} - \frac{28\pi}{15} - \frac{256}{2925\sqrt{1-\tilde{k}}\tilde{k}^4} \\
& - \frac{64}{135\tilde{k}^3} + \frac{3968}{8775\sqrt{1-\tilde{k}}\tilde{k}^3} - \frac{2176}{8775\sqrt{1-\tilde{k}}\tilde{k}^2} + \frac{28}{3\tilde{k}} - \frac{16496}{1755\sqrt{1-\tilde{k}}\tilde{k}} - \frac{2\tilde{k}}{3} \\
& + \frac{64\tilde{k}}{351\sqrt{1-\tilde{k}}} - \frac{128\tilde{k}^2}{351\sqrt{1-\tilde{k}}} + \frac{\tilde{k}^3}{36} + \frac{112\log[1+\sqrt{1-\tilde{k}}]}{15} - \frac{56\log\tilde{k}}{15}
\end{aligned} & \text{for}\quad 0 \le \tilde{k} \le 1 \\[2ex]
\begin{aligned}
& -\frac{16304}{1755\sqrt{-1+\tilde{k}}} - \frac{512}{2925\tilde{k}^5} - \frac{512}{2925\sqrt{-1+\tilde{k}}\tilde{k}^5} + \frac{256}{2925\sqrt{-1+\tilde{k}}\tilde{k}^4} \\
& - \frac{64}{135\tilde{k}^3} - \frac{3968}{8775\sqrt{-1+\tilde{k}}\tilde{k}^3} + \frac{2176}{8775\sqrt{-1+\tilde{k}}\tilde{k}^2} + \frac{28}{3\tilde{k}} + \frac{16496}{1755\sqrt{-1+\tilde{k}}\tilde{k}} - \frac{2\tilde{k}}{3} \\
& - \frac{64\tilde{k}}{351\sqrt{-1+\tilde{k}}} + \frac{128\tilde{k}^2}{351\sqrt{-1+\tilde{k}}} + \frac{\tilde{k}^3}{36} - \frac{56\arctan\left[\frac{1}{\sqrt{-1+\tilde{k}}}\right]}{15} + \frac{56\arctan\left[\sqrt{-1+\tilde{k}}\right]}{15}
\end{aligned} & \text{for}\quad 1 \le \tilde{k} \le 2
\end{cases}
.
$$

**A7**   $n_B = -5/2$

$$
|\rho_B(k)|^2_{n_B=-5/2} = \frac{A^2 k_*^5}{512\pi^4 k_D^2}\left[ -\frac{32}{75\sqrt{|1-\tilde{k}|}} + \frac{272}{25\sqrt{|1-\tilde{k}|}\tilde{k}^2} + \frac{88}{15\tilde{k}} - \frac{848}{75\sqrt{|1-\tilde{k}|}\tilde{k}} - \frac{4\tilde{k}}{5} + \frac{64\tilde{k}}{75\sqrt{|1-\tilde{k}|}} + \frac{\tilde{k}^3}{25} \right]
$$

$$
\begin{aligned}
|\Pi_B^{(V)}(k)|^2_{n_B=-5/2} = \frac{A^2 k_*^5}{256\pi^4 k_D^2}\Bigg[ & -\frac{32}{231\sqrt{|1-\tilde{k}|}} - \frac{1024}{1155\tilde{k}^5} + \frac{1024}{1155\sqrt{|1-\tilde{k}|}\tilde{k}^5} - \frac{512}{1155\sqrt{|1-\tilde{k}|}\tilde{k}^4} + \frac{32}{105\tilde{k}^3} \\
& -\frac{32}{77\sqrt{|1-\tilde{k}|}\tilde{k}^3} + \frac{896}{165\sqrt{|1-\tilde{k}|}\tilde{k}^2} + \frac{44}{15\tilde{k}} - \frac{6464}{1155\sqrt{|1-\tilde{k}|}\tilde{k}} - \frac{\tilde{k}}{5} + \frac{64\tilde{k}}{231\sqrt{|1-\tilde{k}|}} \Bigg]
\end{aligned}
$$

$$
\begin{aligned}
|\Pi_B^{(T)}(k)|^2_{n_B=-5/2} = \frac{A^2 k_*^5}{256\pi^4 k_D^2}\Bigg[ & \frac{1984}{5775\sqrt{|1-\tilde{k}|}} + \frac{512}{1155\tilde{k}^5} - \frac{512}{1155\sqrt{|1-\tilde{k}|}\tilde{k}^5} + \frac{256}{1155\sqrt{|1-\tilde{k}|}\tilde{k}^4} + \frac{64}{105\tilde{k}^3} \\
& -\frac{128}{231\sqrt{|1-\tilde{k}|}\tilde{k}^3} + \frac{117728}{5775\sqrt{|1-\tilde{k}|}\tilde{k}^2} + \frac{28}{3\tilde{k}} - \frac{37088}{1925\sqrt{|1-\tilde{k}|}\tilde{k}} + \frac{2\tilde{k}}{5} - \frac{3968\tilde{k}}{5775\sqrt{|1-\tilde{k}|}} + \frac{\tilde{k}^3}{100} \Bigg]
\end{aligned}
$$

## APPENDIX B: SCALAR PART OF THE LORENTZ FORCE

In order to compute the scalar contribution of a SB of PMFs to the cosmological perturbations, the convolution for the scalar part of the Lorentz Force power spectrum is also necessary. The scalar anisotropic stress can be obtained directly from its relation with the Lorentz force and the magnetic energy density in Eq.(4.21) . We report here the result for the Lorentz force convolution:

$$
|L(k)|^2 = \frac{1}{1024\pi^5 a^8} \int \; d^3p \quad P_B(p)\, P_B(|\mathbf{k}-\mathbf{p}|)[1 + \mu^2 + 4\gamma\beta(\gamma\beta - \mu)], \tag{B1}
$$

with the magnetic field power spectrum in Eq. (2.5) for particular values of $n_B$.

**B1**   $n_B = 3$

$$
|L(k)|^2_{n_B=3} = \frac{A^2 k_D^9}{512\pi^4 k_*^6}
\begin{cases}
\frac{44}{135} - \frac{2\tilde{k}}{3} + \frac{556\tilde{k}^2}{735} - \frac{4\tilde{k}^3}{9} + \frac{164\tilde{k}^4}{1575} + \frac{4\tilde{k}^6}{2079} - \frac{11\tilde{k}^9}{11025} & \text{for}\quad 0 \le \tilde{k} \le 1 \\[1.5ex]
\begin{aligned}
& -\frac{44}{135} + \frac{64}{24255\tilde{k}^5} - \frac{16}{945\tilde{k}^3} + \frac{88}{525\tilde{k}} + \frac{2\tilde{k}}{3} - \\
& \frac{556\tilde{k}^2}{735} + \frac{4\tilde{k}^3}{9} - \frac{164\tilde{k}^4}{1575} - \frac{4\tilde{k}^6}{2079} + \frac{11\tilde{k}^9}{33075}
\end{aligned} & \text{for}\quad 1 \le \tilde{k} \le 2
\end{cases}
.
$$

**B2**   $n_B = 2$

$$
|L(k)|^2_{n_B=2} = \frac{A^2 k_D^7}{512\pi^4 k_*^4}\left[ \frac{44}{105} - \frac{2\tilde{k}}{3} + \frac{8\tilde{k}^2}{15} - \frac{\tilde{k}^3}{6} - \frac{\tilde{k}^5}{240} + \frac{13\tilde{k}^7}{6720} \right].
$$

**B3**  $n_B = 1$

$$|L(k)|^2_{n=1} = \frac{A^2 k_D^5}{512\pi^4 k_*^2} \begin{cases} \frac{44}{75} - \frac{2\tilde{k}}{3} + \frac{32\tilde{k}^2}{105} + \frac{4\tilde{k}^4}{315} - \frac{k^5}{25} & \text{for} \quad 0 \le \tilde{k} \le 1 \\ -\frac{44}{75} + \frac{64}{1575\tilde{k}^5} - \frac{16}{105\tilde{k}^3} + \frac{8}{15\tilde{k}} + \frac{2\tilde{k}}{3} - \frac{32\tilde{k}^2}{105} - \frac{4\tilde{k}^4}{315} + \frac{\tilde{k}^5}{75} & \text{for} \quad 1 \le \tilde{k} \le 2 \end{cases}.$$

**B4**  $n_B = 0$

$$|L(k)|^2_{n_B=0} = \frac{A^2 k_D^3}{512\pi^4} \left[ \frac{43}{48} - \frac{1}{16\tilde{k}^4} - \frac{1}{32\tilde{k}^3} + \frac{7}{48\tilde{k}^2} + \frac{13}{192\tilde{k}} - \frac{67\tilde{k}}{96} + \frac{\tilde{k}^2}{48} + \frac{17\tilde{k}^3}{384} - \frac{\log|1-k|}{16\tilde{k}^5} \right.$$
$$\left. + \frac{\log|1-k|}{6\tilde{k}^3} - \frac{\log|1-k|}{8\tilde{k}} + \frac{\tilde{k}^3 \log|1-k|}{48} \right].$$

**B5**  $n_B = -1$

$$|L(k)|^2_{n_B=-1} = \frac{A^2 k_D k_*^2}{512\pi^4} \begin{cases} \frac{44}{15} - 2\tilde{k} - \frac{4\tilde{k}^2}{105} & \text{for} \quad 0 \le \tilde{k} \le 1 \\ -\frac{44}{15} - \frac{64}{105\tilde{k}^5} + \frac{16}{15\tilde{k}^3} + \frac{8}{3\tilde{k}} + \frac{2\tilde{k}}{3} + \frac{4\tilde{k}^2}{105} & \text{for} \quad 1 \le \tilde{k} \le 2 \end{cases}.$$

**B6**  $n_B = -3/2$

$$|L(k)|^2_{n=-3/2} = \frac{A^2 k_*^3}{512\pi^4} \begin{cases} \frac{10616}{1755\sqrt{1-\tilde{k}}} - \frac{2048}{2925\tilde{k}^5} + \frac{2048}{2925\sqrt{1-\tilde{k}}\tilde{k}^5} - \frac{22\pi}{15} + \frac{128}{135\tilde{k}^3} - \frac{9088}{8775\sqrt{1-\tilde{k}}\tilde{k}^3} \\ + \frac{88}{15\tilde{k}} - \frac{10136}{1775\sqrt{1-\tilde{k}}\tilde{k}} + \frac{32\tilde{k}}{1775\sqrt{1-\tilde{k}}} - \frac{64\tilde{k}^2}{1775\sqrt{1-\tilde{k}}} + \frac{88\log[1+\sqrt{1-\tilde{k}}]}{15} - \frac{44\log\tilde{k}}{15} & \text{for} \quad 0 \le \tilde{k} \le 1 \\ -\frac{10616}{1755\sqrt{-1+\tilde{k}}} - \frac{2048}{2925\tilde{k}^5} - \frac{2048}{2925\sqrt{-1+\tilde{k}}\tilde{k}^5} + \frac{1024}{2925\sqrt{-1+\tilde{k}}\tilde{k}^4} \\ + \frac{128}{135\tilde{k}^3} + \frac{9088}{8775\sqrt{-1+\tilde{k}}\tilde{k}^3} - \frac{3776}{8775\sqrt{-1+\tilde{k}}\tilde{k}^2} + \frac{88}{15\tilde{k}} + \frac{10136}{1775\sqrt{-1+\tilde{k}}\tilde{k}} \\ - \frac{32\tilde{k}}{1775\sqrt{-1+\tilde{k}}} + \frac{64\tilde{k}^2}{1775\sqrt{-1+\tilde{k}}} - \frac{44\arctan\left[\frac{1}{\sqrt{-1+\tilde{k}}}\right]}{15} + \frac{44\arctan\left[\sqrt{-1+\tilde{k}}\right]}{15} & \text{for} \quad 1 \le \tilde{k} \le 2 \end{cases}.$$

**B7**  $n_B = -5/2$

$$|L(k)|^2_{n_B=-5/2} = \frac{A^2 k_*^5}{512\pi^4 k_D^2} \left[ -\frac{32}{1155\sqrt{|1-\tilde{k}|}} + \frac{2048}{1155\tilde{k}^5} - \frac{2048}{1155\sqrt{|1-\tilde{k}|}\tilde{k}^5} + \frac{1024}{1155\sqrt{|1-\tilde{k}|}\tilde{k}^4} - \frac{128}{105\tilde{k}^3} \right.$$
$$\left. + \frac{1664}{1155\sqrt{|1-\tilde{k}|}\tilde{k}^3} + \frac{12976}{1155\sqrt{|1-\tilde{k}|}\tilde{k}^2} + \frac{88}{15\tilde{k}} - \frac{13648}{1155\sqrt{|1-\tilde{k}|}\tilde{k}} + \frac{64\tilde{k}}{1155\sqrt{|1-\tilde{k}|}} \right]$$

## REFERENCES

Abramowitz M. and Stegun I., *Handbook of mathematical functions with formulas, graphs, and mathematical table*, New York: Dover Publishing (1965).

Brown I. and Crittenden R., Phys. Rev. D **72** (2005) 063002

Caprini C., Durrer R. and Kahniashvili T., Phys. Rev. D **69** (2004) 063006

Durrer R., "Cosmic Magnetic Fields and the CMB", New Astron. Rev. **51** (2007) 275 [arXiv:astro-ph/0609216].

Durrer R.,Ferreira P.G. and Kahniashvili T.,Phys. Rev. D **61** (2000) 043001

Finelli F., Paci F., Paoletti D., 2008, Phys. Rev. D, **78**,(2008) 023510

Giovannini M. and Kunze K.E.,Phys. Rev. D**77** (2008) 063003

Kahniashvili T. and Ratra B., Phys. Rev. D **75**,(2006) 023002

Koh S., and Lee C.H., Phys. Rev. D **62**, (2000) 083509.

Lewis A., Phys. Rev. D, **70**,(2004) 043011

Lewis A., Challinor A. and Lasenby A., Astrophys. J. **538** (2000) 473

Ma C. P. and Bertschinger E., Ap. J., 455 (1995) 7.

Mack A., Kahniashvili T., Kosowsky A., Phys. Rev. D, **65**,(2002) 123004

[Planck Collaboration], "Planck: The scientific programme," arXiv:astro-ph/0604069 (2006).

Seshadri T. R and Subramanian K., Phys. Rev. Lett. **87** (2001) 101301

Subramanian K., "Magnetizing the Universe", arXiv:astro-ph/0802.2804 [astro-ph]

Subramanian K. and Barrow J. D., Phys. Rev. Lett. **81** (1998) 3575

Yamazaki D. G., Ichiki K., Kajino T., and Mathews G.J., apj, 646, 719 (2006).